Cucurbituril - ferrocene: host - guest based pretargeted positron emission tomography in a xenograft model

Vilma IJ Jallinoja[1,2], **Brandon D Carney**[1,2], **Meiying Zhu**[1], **Kavita Bhatt**[2], **Paul J Yazaki**[3], **Jacob L Houghton**[1,2,*]

[1]Department of Radiology and Radiological Sciences, Vanderbilt University Medical Center, Nashville, Tennessee, 37232, USA.

[2]Department of Radiology, Stony Brook University, Stony Brook, New York, 11774, USA.

[3]Beckman Institute, City of Hope, Duarte, California 91010, USA.

Abstract

Pretargeted positron emission tomography is a macromolecule driven nuclear medicine technique that involves targeting a pre-administered antigen target-bound macromolecule with a radioligand *in vivo*, aiming to minimize the overall radiation dose. This study investigates the use of antibody based host-guest chemistry methodology for pretargeted positron emission tomography. We hypothesize that the novel pretargeting approach reported here overcomes the challenges the current pretargeting platforms have with the *in vivo* stability and modularity of the pretargeting components. A cucurbit[7]uril host molecule modified, anti-carcinoembryonic antigen antibody (M5A; CB7-M5A) and a ^{68}Ga-radiolabeled ferrocene guest radioligand ([^{68}Ga]Ga-NOTA-PEG$_3$-NMe$_2$-Fc) were studied as potential host-guest chemistry pretargeting agents for positron emission tomography in BxPC3 xenografted nude mice. The viability of the platform was studied via *in vivo* biodistribution and positron emission tomography. Tumor uptake of [^{68}Ga]Ga-NOTA-PEG$_3$-NMe$_2$-Fc was significantly higher in mice which received CB7-M5A prior to the radioligand injection (pretargeted), (3.3 ± 0.7 %ID/g) compared to mice which only received the radioligand (non-pretargeted), (0.2 ± 0.1 %ID/g).

Graphical Abstract

---

*Corresponding author: Jacob Houghton, PhD, Stony Brook University Cancer Center, 100 Nicolls Rd, Stony Brook, NY 11774, Tel: 6153226215, Fax: 6314447538, jacob.houghton@stonybrookmedicine.edu.
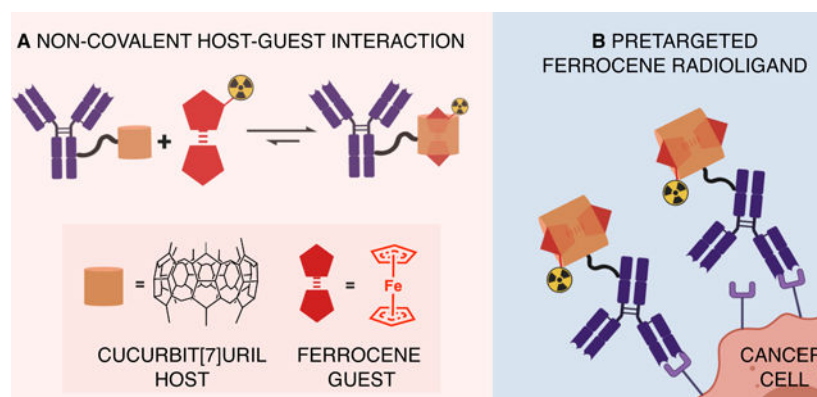
INTRODUCTION

The purpose of the pretargeting approach is to decrease the overall radiation dose received in biomacromolecule-based nuclear medicine procedures. In pretargeted imaging or radiotherapy, a tumor-targeting macromolecule is administered prior to a radioactive small molecule (radioligand) which is designed to interact with the macromolecule with high specificity.[1–3] (Figure 1) Several approaches for pretargeting have been investigated in which the pretargeting interaction occurs via specific intra- or intermolecular forces.

Of the four most prominent pretargeting platforms reported, the two most promising are based on either click-chemistry (inverse electron demand Diels-Alder, IEDDA) or bispecific antibody-hapten methodologies. However, in the IEDDA approach, the *trans*-cyclooctene (TCO) that is appended to the antibody has a biological half-life of 1–10 days in mouse models, depending on the chemical structure TCO-conjugate,[4,5] which limits the interval time between administration of targeting molecule and the radioligand. Using the IEDDA pretargeting platform, extended interval times have shown to result in compromised tumor uptake.[6,7] The main drawback of the bispecific antibody (bsAb)-hapten approach is the lack of modularity, requiring the development of a new modified bsAb for every tumor antigen.[8] Furthermore, in clinical trials of the bsAb-hapten platform, immunogenicity of the pretargeting agents has been an issue when anti-inflammatory drugs are not used as part of the pretargeting scheme.[9–11] The other two platforms that have been reported are based on streptavidin-biotin binding or oligonucleotide hybridization as the pretargeting interaction. The clinical viability of the streptavidin-biotin methodology is hindered by problems with immunogenicity and the need to use clearing agents.[12,13] Finally, the nucleotide hybridization driven pretargeting platform, studied only in preclinical models, has suffered from poor tumor uptake (%ID/g) when full length antibodies are used for targeting.[14–16] While full-length antibodies are currently the primary and most attractive targeting vectors for pretargeting, the nucleotide hybridization approach has shown encouraging results with affibody targeting vectors, suggesting they represent a potentially fruitful alternative.[17–19]

Here we present a host-guest based pretargeting approach, which we hypothesize overcomes many of the challenges observed in other pretargeting platforms. Our approach utilizes a cucurbit[7]uril (CB7) host modified carcinoembryonic antigen (CEA) targeting antibody (M5A; CB7-M5A) and a ^{68}Ga-radiolabeled ferrocene (Fc) guest radioligand. CB7 is a macrocyclic host compound that has high affinity for Fc based compounds.[20] Fc molecules with adjacent positively charged substituents form stronger complexes with CB7 ($K \approx 10^{12}$–10^{15} M^{-1}) compared to neutral Fc derivatives ($K \approx 10^9$ M^{-1}).[20] In contrast to other pretargeting approaches, the antibody bound pretargeting host moiety (CB7) is stable *in vivo*.[21] The ferrocene does oxidize to ferrocenium *in vivo*, though this does not hinder the host-guest complex formation.[22,23] Essentially any tumor targeting antibody can be modified with a CB7-moiety and the Fc-ligand can be modified to carry a variety of different diagnostic or therapeutic radionuclides.

RESULTS AND DISCUSSION

Development and characterization of host-guest pretargeting components

To test the host-guest, CB7-Fc driven pretargeted positron emission tomography (PET) *in vivo*, we first developed a CB7 conjugated M5A antibody (CB7-M5A). M5A antibody (hT84.66-M5A) is a humanized, CEA-targeting IgG, whose murine counterpart has shown minimal internalization[24] as have many other CEA targeting antibodies.[25] Using the antibody's surface lysine residues, we first functionalized the M5A with a *N*-hydroxysuccinimide dibenzocyclooctyne (DBCO) moiety and followed this by reacting the DBCO with an azide functionalized CB7 group through click chemistry. Each antibody molecule was determined to have an average of 0.77 ± 0.01 CB7-moieties. The immunoreactive fraction of the CB7-M5A was determined to be 95.7 ± 0.7% by Lindmo assay[26,27] using the CEA expressing adenocarcinoma cell line, BxPC3.[28] As for the secondary pretargeting agent, the Fc-functionalized radioligand, [^{68}Ga]Ga-NOTA-PEG$_3$-NMe$_2$-Fc (**1**) was synthesized in four steps (Figure 2). The overall chemical yield of the precursor NOTA-PEG$_3$-NMe$_2$-Fc (**4**) reaction was 20.3% with final chemical purity of 95.6%. The radiochemical yield of the [^{68}Ga]Ga-NOTA-PEG$_3$-NMe$_2$-Fc radiosynthesis, was 78.3 ± 10.2% and its final radiochemical purity was determined to be 96.7 ± 2.4% (n=4).

The blood half-life, *in vitro* stability, and distribution coefficient (log D) of the radioligand (**1**) was determined using a longer lived analogue of the radioligand, [^{67}Ga]Ga-NOTA-PEG$_3$-NMe$_2$-Fc (**5**). Compound **5** was synthesized similar to compound **1** (Figure 2) resulting in 33.9 ± 13.2% radiochemical yield with a final radiochemical purity of 95.5 ± 0.4% (n=4). Compound **5** was stable up to four hours, showing 91.2 ± 1.5% intact at 2 h and 86.6 ± 0.7% at 4 h in PBS (pH 7.4) at 37 °C. The log D of the radioligand was studied with the shake-flask method in 1:1 (v/v) of 1-octanol and PBS (pH 7.4) to be −3.2 ± 0.1. Finally the blood half-life of the radioligand was determined as 10.0 minutes by saphenous vein blood draw in healthy mice at six timepoints over a 60-minute period (Figure S2).

Establishing the *in vivo* behavior of the M5A antibody in tumor bearing mice

The pharmacokinetics of the M5A antibody was interrogated in BxPC3 tumor bearing mice using directly radiolabeled M5A ([^{89}Zr]Zr-DFO-M5A). For this purpose, isothiocyanate

functionalized deferoxamine (DFO) was conjugated to M5A via the lysine residues. The modified antibody was produced with an overall yield of 86.0% and was radiolabeled with $[^{89}Zr]Zr(C_2O_4)_2$ resulting in a radiochemical yield of $81.5 \pm 7.6\%$, a radiochemical purity >99%, and molar activity of 8.2 MBq/nmol (n=3). Immunoreactivity of the $[^{89}Zr]Zr$-DFO-M5A was found to be $89.6 \pm 2.07\%$ (n=3) via Lindmo cellular binding assay using the BxPC3 cell line.

$[^{89}Zr]Zr$-DFO-M5A was studied *in vivo* in two cohorts of male nude mice bearing BxPC3 xenografts on their right flank. The experimental cohort received $[^{89}Zr]Zr$-DFO-M5A (1.85 MBq/nmol, 1 nmol) while the control group received a 2-fold blocking dose of M5A (0.79 MBq/nmol; 2.3 nmol). Both cohorts were sacrificed for *ex vivo* biodistribution at 72 h post injection. The biodistribution data (Figure 3A) shows the tumor uptake was significantly lower in the control group (18.6 ± 5.1 %ID/g) compared to the experimental group (31.8 ± 5.8 %ID/g) (p=0.026).

A separate cohort of mice were used for a PET imaging study of $[^{89}Zr]Zr$-DFO-M5A. The mice received $[^{89}Zr]Zr$-DFO-M5A (7.4 MBq/nmol; 1 nmol) via the tail vein 72 hours before imaging (Figure 3B). The image data corroborated the biodistribution data at 72 h timepoint, showing the tumor uptake with some residual blood pool signal and also some signal in clearance organs such as the liver.

In vivo host-guest pretargeting in tumor bearing mice

The purpose of our *in vivo* pretargeting experiments was to investigate the ability of $[^{68}Ga]Ga$-NOTA-PEG_3-NMe_2-Fc to bind specifically to CB7-M5A in a xenograft model. The goals of this study did not include optimization of the pretargeting parameters, but rather were focused on establishing the feasibility of the CB7-Fc based pretargeting. The pretargeting studies included four cohorts of BxPC3 tumor-bearing female nude mice. Three experimental cohorts received CB7-M5A 72 hours prior to the $[^{68}Ga]Ga$-NOTA-PEG_3-NMe_2-Fc administration and the cohorts were sacrificed at 1, 2 and 4 h post radioligand injection for *ex vivo* biodistribution. One of the cohorts (4 hour timepoint) was imaged at 2 and 4 h post radioligand injection. The fourth cohort serving as a control group, received only the $[^{68}Ga]Ga$-NOTA-PEG_3-NMe_2-Fc, was euthanized for *ex vivo* biodistribution study 2 h post radioligand administration. Tumor uptake was significantly higher at 2 hours post injection in the pretargeting group (3.3 ± 0.7 %ID/g) compared to control (p=0.021) (Figure 4). Uptake in the liver, kidney and small intestine decreased over the 4-hour study period while uptake in the large intestine rose after 2 hours.

The PET imaging showed excretion through the bladder and hepatobiliary system, which coupled with the location of the tumor resulted in poor visualization of the tumor 2 hours post radioligand injection in two of three mice at the 2 hour time point. However, after 4 hours, we were able to observe the tumor mass for all mice (Figure 5 & Figure S7).

In this study we have shown that the pretargeted Fc-radioligand was successfully delivered to tumor tissue and that it stayed bound to the CB7 during the 4 hour post injection time period. This also shows that CB7-M5A stayed bound at the tumor site and that the CB7 moieties were still present 72 hours after administration. There is no murine

counterpart of human CEA expressed in mice,[29] so signal in non-tumor tissue originated from free radioligand. This was verified by the biodistribution of the non-pretargeted ligand. Additionally the biodistribution of [^{89}Zr]Zr-DFO-M5A showed significant difference in only the tumor uptake between blocked and non-blocked cohorts.

The presented pretargeting approach resulted in modest tumor uptake (%ID/g). However, the approach could be improved through optimization of different pretargeting parameters (e.g. interval time and pretargeting agents' dosing) and further optimization of the radioligand's structure. For other pretartgeting approaches, this kind of optimization has resulted in improved tumor uptake and tumor-to-background.[30–32] Furthermore, [^{89}Zr]Zr-DFO-M5A had tumor uptake of only 31.8 ± 5.8 %ID/g at the pretargeting time point of 72 hours, which is relatively modest compared to some of the other antibodies that have been used in pretargeting.[6,33] Pretargeting with M5A has yet to be reported with other systems so this novel approach cannot yet be directly compared to other pretargeting approaches. Studies to directly comparing this novel approach to others (e.g. IEDDA pretargeting) are currently underway in our laboratory, as are studies investigating CB7-adamantane pretargeting, another host-guest pair with the potential for pretargeting applications.[34] Herein, we have substantially expanded upon the reported work and successfully performed CB7-Fc pretargeted PET imaging in xenograft models. Additionally, we have shown that the CB7-Fc complex is stable at the tumor site over the course of the 4 hour time period. Further development of the chemical structure of the Fc-radioligand will be performed to optimize its pharmacokinetics.

Supplementary Material

Refer to Web version on PubMed Central for supplementary material.

ACKNOWLEDGMENT

REFERENCES

1. Bailly C, Bodet-Milin C, Rousseau C, Faivre-Chauvet A, Kraeber-Bodéré F, Barbet J (2017) Pretargeting for imaging and therapy in oncological nuclear medicine. EJNMMI Radiopharm. Chem 2,6. DOI: 10.1186/s41181-017-0026-8.

2. Stéen EJL, Edem PE, Nørregaard K, Jørgensen JT, Shalgunov V, Kjaer A, Herth MM (2018) Pretargeting in nuclear imaging and radionuclide therapy: Improving efficacy of theranostics and nanomedicines. Biomaterials 179, 209–245. DOI: 10.1016/j.biomaterials.2018.06.021. [PubMed: 30007471]

3. van de Watering FCJ, Rijpkema M, Robillard M, Oyen WJG, Boerman OC (2014) Pretargeted imaging and radioimmunotherapy of cancer using antibodies and bioorthogonal chemistry. Front. Med 1,44. DOI: 10.3389/fmed.2014.00044.

4. Rossin R, van den Bosch SM, ten Hoeve W, Carvelli M, Versteegen RM, Lub J, Robillard MS (2013) Highly Reactive trans-Cyclooctene Tags with Improved Stability for Diels–Alder Chemistry

in Living Systems. Bioconjug. Chem 24, 1210–1207. DOI: 10.1021/bc400153y. [PubMed: 23725393]

5. Rossin R, van Duijnhoven SMJ, Läppchen T, van den Bosch SM, Robillard MS (2014) Trans-cyclooctene tag with improved properties for tumor pretargeting with the diels-alder reaction. Mol. Pharm 11, 3090–3096. DOI: 10.1021/mp500275a. [PubMed: 25077373]

6. Membreno R, Cook BE, Fung K, Lewis JS, Zeglis BM (2018) Click-Mediated Pretargeted Radioimmunotherapy of Colorectal Carcinoma. Mol. Pharm 15, 1729–1734. DOI: 10.1021/acs.molpharmaceut.8b00093. [PubMed: 29502416]

7. Cook BE, Adumeau P, Membreno R, Carnazza KE, Brand C, Reiner T, Agnew BJ, Lewis JS, Zeglis BM (2016) Pretargeted PET Imaging Using a Site-Specifically Labeled Immunoconjugate. Bioconjug. Chem 27, 1789–1795. DOI: 10.1021/acs.bioconjchem.6b00235. [PubMed: 27356886]

8. Labrijn AF, Janmaat ML, Reichert JM, Parren PWHI (2019) Bispecific antibodies: a mechanistic review of the pipeline. Nat. Rev. Drug Discov 18, 585–608. DOI: 10.1038/s41573-019-0028-1. [PubMed: 31175342]

9. Barbet J, Peltier P, Bardet S, Vuillez JP, Bachelot S, Denet P, Olivier F, Leccia B, Corcuff D, Huglo C et al. (1998) Radioimmunodetection of medullary thyroid carcinoma using indium-111 bivalent hapten and anti-CEA x anti-DTPA-indium bispecific antibody. J. Nucl. Med 39, 1172–1178. [PubMed: 9669389]

10. Chatal JF, Campion L, Kraeber-Bodéré F, Bardet S, Vuillez JP, Charbonnel B, Rohmer V, Chang CH, Sharkey RM, Goldenberg DM, et al. (2006) Survival improvement in patients with medullary thyroid carcinoma who undergo pretargeted anti-carcinoembryonic-antigen radioimmunotherapy: a collaborative study with the French Endocrine Tumor Group. J. Clin. Oncol 24, 1705–1711. DOI: 10.1200/JCO.2005.04.4917. [PubMed: 16549819]

11. Rousseau C, Goldenberg DM, Colombié M, Sébille JC, Meingan P, Ferrer L, Baumgartner P, Cerato E, Masson D, Campone M, et al. (2020) Initial Clinical Results of a Novel Immuno-PET Theranostic Probe in Human Epidermal Growth Factor Receptor 2-Negative Breast Cancer. J. Nucl. Med 61, 1205–1211. DOI: 10.2967/jnumed.119.236000. [PubMed: 32169921]

12. Forero-Torres A, Shen S, Breitz H, Sims RB, Axworthy DB, Khazaeli MB, Chen KH, Percent I, Besh S, LoBuglio AF, et al. (2005) Pretargeted Radioimmunotherapy (RIT) with a Novel Anti-TAG-72 Fusion Protein. Cancer Biother. Radiopharm 20, 379–390. DOI: 10.1089/cbr.2005.20.379. [PubMed: 16114986]

13. Weiden PL, Breitz HB (2001) Pretargeted radioimmunotherapy (PRIT) for treatment of non-Hodgkin's lymphoma (NHL). Crit. Rev. Oncol. Hematol 40, 37–51. DOI: 10.1016/s1040-8428(01)00133-0. [PubMed: 11578915]

14. Leonidova A, Foerster C, Zarschler K, Schubert M, Pietzsch HJ, Steinbach J, Bergmann R, Metzler-Nolte N, Stephan H, Gasser G (2015) In vivo demonstration of an active tumor pretargeting approach with peptide nucleic acid bioconjugates as complementary system. Chem. Sci 6, 5601–5616. DOI: 10.1039/C5SC00951K. [PubMed: 29861898]

15. Schubert M, Bergmann R, Förster C, Sihver W, Vonhoff S, Klussmann S, Bethge L, Walther M, Schlesinger J, Pietzsch J, Steinbach J, Pietzsch HJ (2017) Novel Tumor Pretargeting System Based on Complementary L-Configured Oligonucleotides. Bioconjugate Chem 28, 1176–1188 DOI: 10.1021/acs.bioconjchem.7b00045.

16. Westerlund K, Vorobyeva A, Mitran B, Orlova A, Tolmachev V, Eriksson Karlström A, Altai M (2019) Site-specific conjugation of recognition tags to trastuzumab for peptide nucleic acid-mediated radionuclide HER2 pretargeting. Biomaterials 203, 73–85. DOI: 10.1016/j.biomaterials.2019.02.012 [PubMed: 30877838]

17. Honarvar H, Westerlund K, Altai M, Sandström M, Orlova A, Tolmachev V, Karlström AE (2016) Feasibility of Affibody Molecule-Based PNA-Mediated Radionuclide Pretargeting of Malignant Tumors. Theranostics 6, 93–103. DOI: 10.7150/thno.12766. [PubMed: 26722376]

18. Tano H, Oroujeni M, Vorobyeva A, Westerlund K, Liu Y, Xu T, Vasconcelos D, Orlov a A., Karlström AE, Tolmachev V (2021) Comparative Evaluation of Novel 177Lu-Labeled PNA Probes for Affibody-Mediated PNA-Based Pretargeting. Cancers 13, 500. DOI: 10.3390/cancers13030500. [PubMed: 33525578]

19. Westerlund K, Altai M, Mitran B, Konijnenberg M, Oroujeni M, Atterby C, de Jong M, Orlova A, Mattsson J, Micke P, et al. (2018) Radionuclide Therapy of HER2-Expressing Human Xenografts

Using Affibody-Based Peptide Nucleic Acid-Mediated Pretargeting: In Vivo Proof of Principle. J. Nucl. Med 59, 1092–1098. DOI: 10.2967/jnumed.118.208348. [PubMed: 29439013]

20. Barrow SJ, Kasera S, Rowland MJ, del Barrio J, Scherman OA (2015) Cucurbituril-Based Molecular Recognition. Chem. Rev 115, 12320–12406. DOI: 10.1021/acs.chemrev.5b00341. [PubMed: 26566008]

21. Masson E, Ling X, Joseph R, Kyeremeh-Mensah L, Lu X (2012) Cucurbituril chemistry: a tale of supramolecular success. RSC. Adv 2, 1213–1247. DOI: 10.1039/C1RA00768H

22. Daum S, Toms J, Reshetnikov V, Özkan HG, Hampel F, Maschauer S, Hakimioun A, Beierlein F, Sellner L, Schmitt M, et al. (2019) Identification of Boronic Acid Derivatives as an Active Form of N-Alkylaminoferrocene-Based Anticancer Prodrugs and Their Radiolabeling with ^{18}F. Bioconjugate Chem 30, 1077–1086. DOI: 10.1021/acs.bioconjchem.9b00019.

23. Ong W, Kaifer AE (2003) Unusual Electrochemical Properties of the Inclusion Complexes of Ferrocinium and Cobaltocenium with Cucurbit[7]uril. Organometallics 22, 4181–4183.

24. Bryan JN, Jia F, Mohsin H, Sivaguru G, Miller WH, Anderson CJ, Henry CJ, Lewis MR (2005) Comparative uptakes and biodistributions of internalizing vs. noninternalizing copper-64 radioimmunoconjugates in cell and animal models of colon cancer. Nucl. Med. Biol 32, 851–858. DOI: 10.1016/j.nucmedbio.2005.05.006. [PubMed: 16253810]

25. Schmidt MM, Thurber GM, Wittrup KD, (2008) Kinetics of anti-carcinoembryonic antigen antibody internalization: effects of affinity, bivalency, and stability. Cancer Immunol. Immunother 57, 1879–1890. DOI: 10.1007/s00262-008-0518-1. [PubMed: 18408925]

26. Lindmo T, Bunn PA Jr (1986) Determination of the true immunoreactive fraction of monoclonal antibodies after radiolabeling. Method. enzymol 121, 678–691. DOI: 10.1016/0076-6879(86)21067-8.

27. Lindmo T, Boven E, Cuttitta F, Fedorko J, Bunn PA Jr (1984) Determination of the immunoreactive fraction of radiolabeled monoclonal antibodies by linear extrapolation to binding at infinite antigen excess. J. Immunol. Methods 72, 77–89. DOI: 10.1016/0022-1759(84)90435-6 [PubMed: 6086763]

28. Girgis MD, Olafsen T, Kenanova V, McCabe KE, Wu AM, Tomlinson JS (2011) Targeting CEA in Pancreas Cancer Xenografts with a Mutated scFv-Fc Antibody Fragment. EJNMMI Res 1,24. DOI: 10.1186/2191-219X-1-24.

29. Hance KW, Zeytin HE, Greiner JW (2005) Mouse models expressing human carcinoembryonic antigen (CEA) as a transgene: Evaluation of CEA-based cancer vaccines. Mutat. Res 576, 132–154. DOI: 10.1016/j.mrfmmm.2004.10.014. [PubMed: 15888344]

30. Membreno R, Keinänen OM, Cook BE, Tully KM, Fung KC, Lewis JS, Zeglis BM (2019) Toward the optimization of Click-Mediated Pretargeted Radioimmunotherapy. Mol. Pharmaceutics 16, 2259–2263.

31. van Rij CM, Lütje S, Frielink C, Sharkey RM, Goldenberg DM, Franssen GM, McBride WJ, Rossi EA, Oyen WJG, Boerman OC (2013) Pretargeted immuno-PET and radioimmunotherapy of prostate cancer with an anti-TROP-2 x anti-HSG bispecific antibody. EJNMMI 40, 1377–1383. DOI: 10.1007/s00259-013-2434-7

32. Meyer JP, Kozlowski P, Jackson J, Cunanan KM, Adumeau P, Dilling TR, Zeglis BM, Lewis JS (2017) Exploring Structural Parameters for Pretargeting Radioligand Optimization. J. Med. Chem 60, 8201–8217. DOI: 10.1021/acs.jmedchem.7b01108. [PubMed: 28857566]

33. Houghton JL, Zeglis BM, Abdel-Atti D, Aggeler R, Sawada R, Agnew BJ, Scholz WW, Lewis JS (2015) Site-specifically labeled CA19.9-targeted immunoconjugates for the PET, NIRF, and multimodal PET/NIRF imaging of pancreatic cancer. PNAS 112, 15850–15855. DOI: 10.1073/pnas.1506542112. [PubMed: 26668398]

34. Strebl MG, Yang J, Isaacs L, Hooker JM (2018) Adamantane/Cucurbituril: A Potential Pretargeted Imaging Strategy in Immuno-PET. Mol. Imaging 17, 1–7. DOI: 10.1177/1536012118799838.
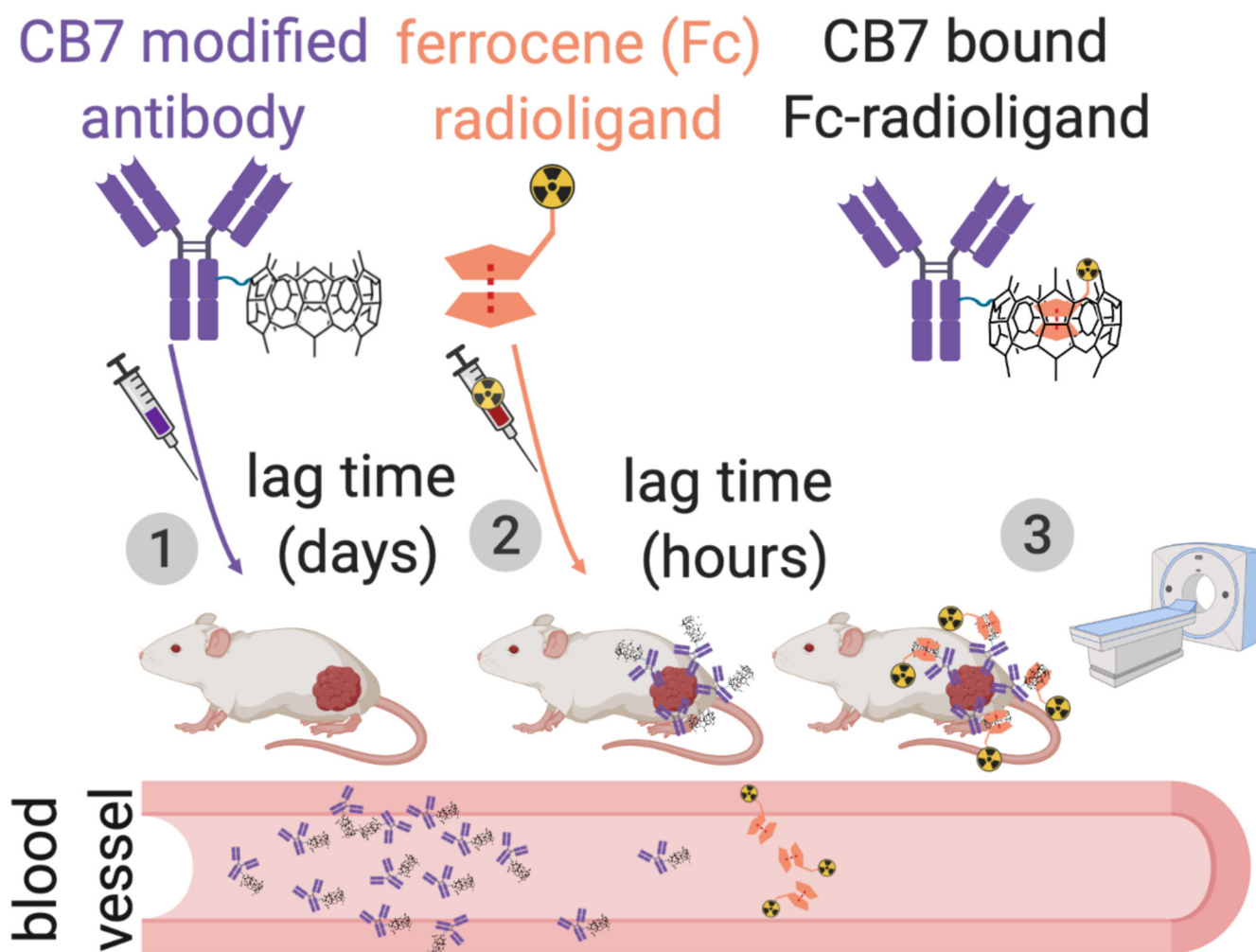
FIGURE 1.
Scheme for host-guest pretargeted nuclear medicine imaging: (1) administration of a cucurbit[7]uril (CB7) modified antibody, (2) administration of the ferrocene (Fc) radioligand several days later and (3) the imaging is performed hours after the radioligand injection.
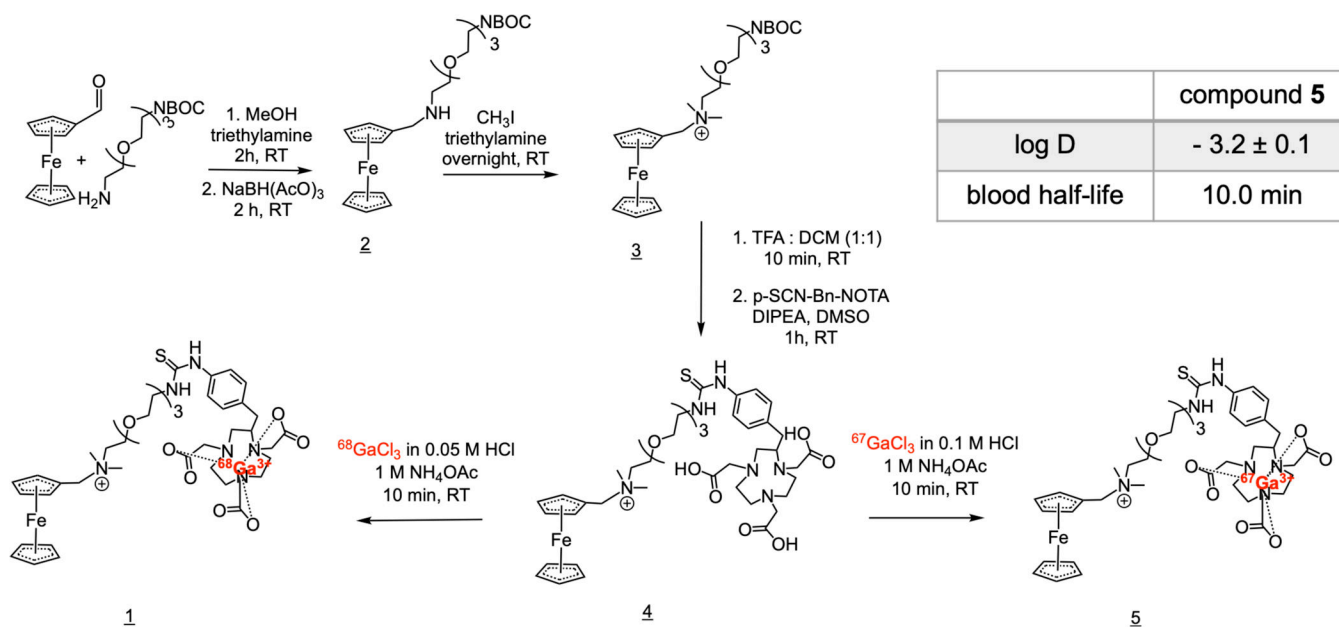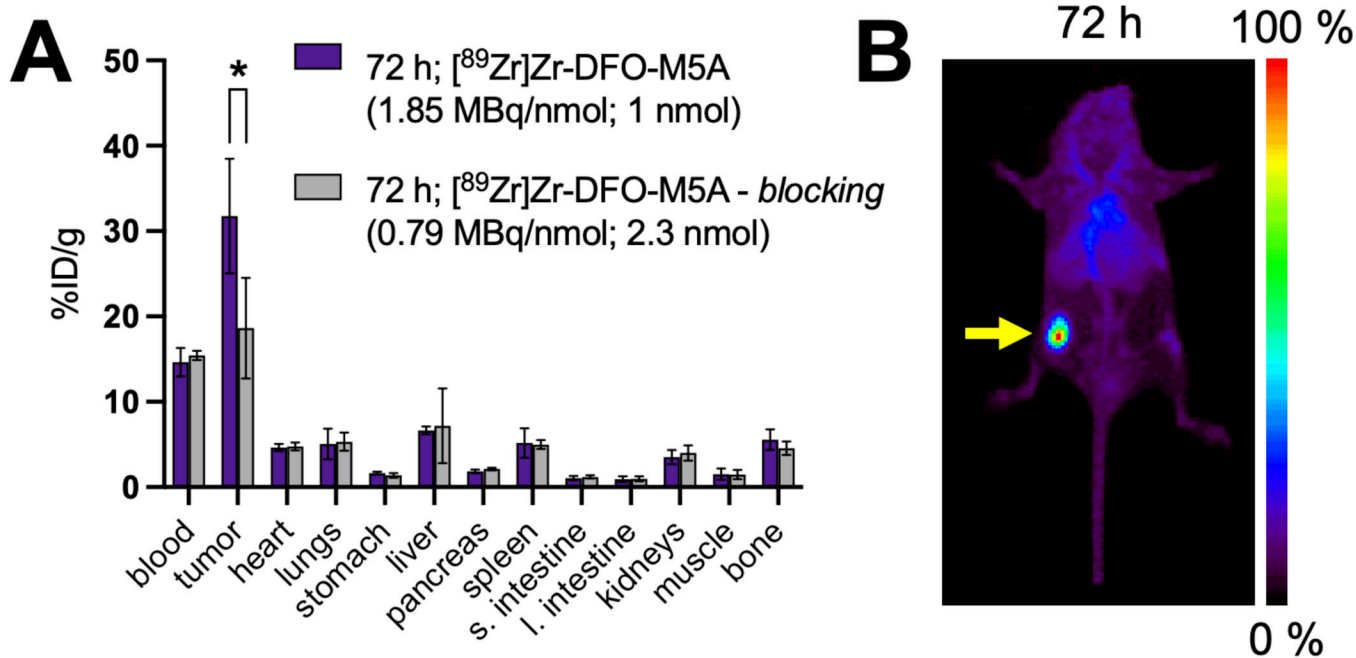
	compound **5**
log D	- 3.2 ± 0.1
blood half-life	10.0 min

FIGURE 2.
Synthesis scheme of [^{68}Ga]Ga-NOTA-PEG$_3$-NMe$_2$-Fc (**1**) and [^{67}Ga]Ga-NOTA-PEG$_3$-NMe$_2$-Fc (**5**).

FIGURE 3.
Activity biodistribution data of [^{89}Zr]Zr-DFO-M5A in BxPC3 tumor bearing nude mice at 72 h post injection. * $p<0.05$ (A) A maximum intensity projection image showing [^{89}Zr]Zr-DFO-M5A biodistribution in a BxPC3 xenografted nude mouse 72 h post injection. Yellow arrow indicates the location of the tumor. (B)

FIGURE 4.
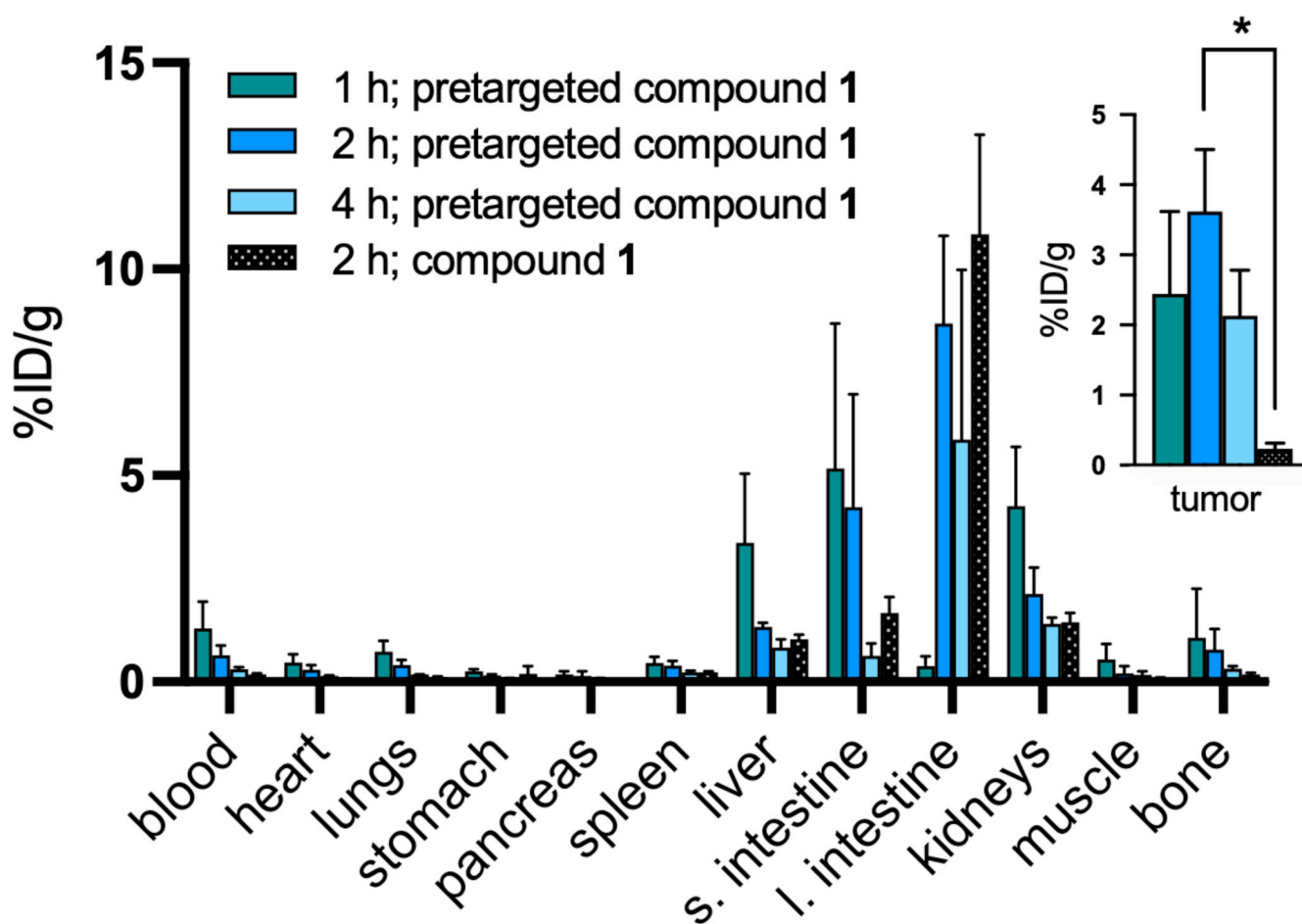Biodistribution data for $[^{68}Ga]Ga\text{-}NOTA\text{-}PEG_3\text{-}NMe_2\text{-}Fc$ (**1**) in BxPC3 tumor bearing mice. Mice received either CB7-M5A 72 hours prior to the radioligand administration (pretargeted; green, blue, light blue) or the radioligand without CB7-M5A (non-pretargeted; black). The time values represent the amount of time after the radioligand administration. * $p < 0.05$
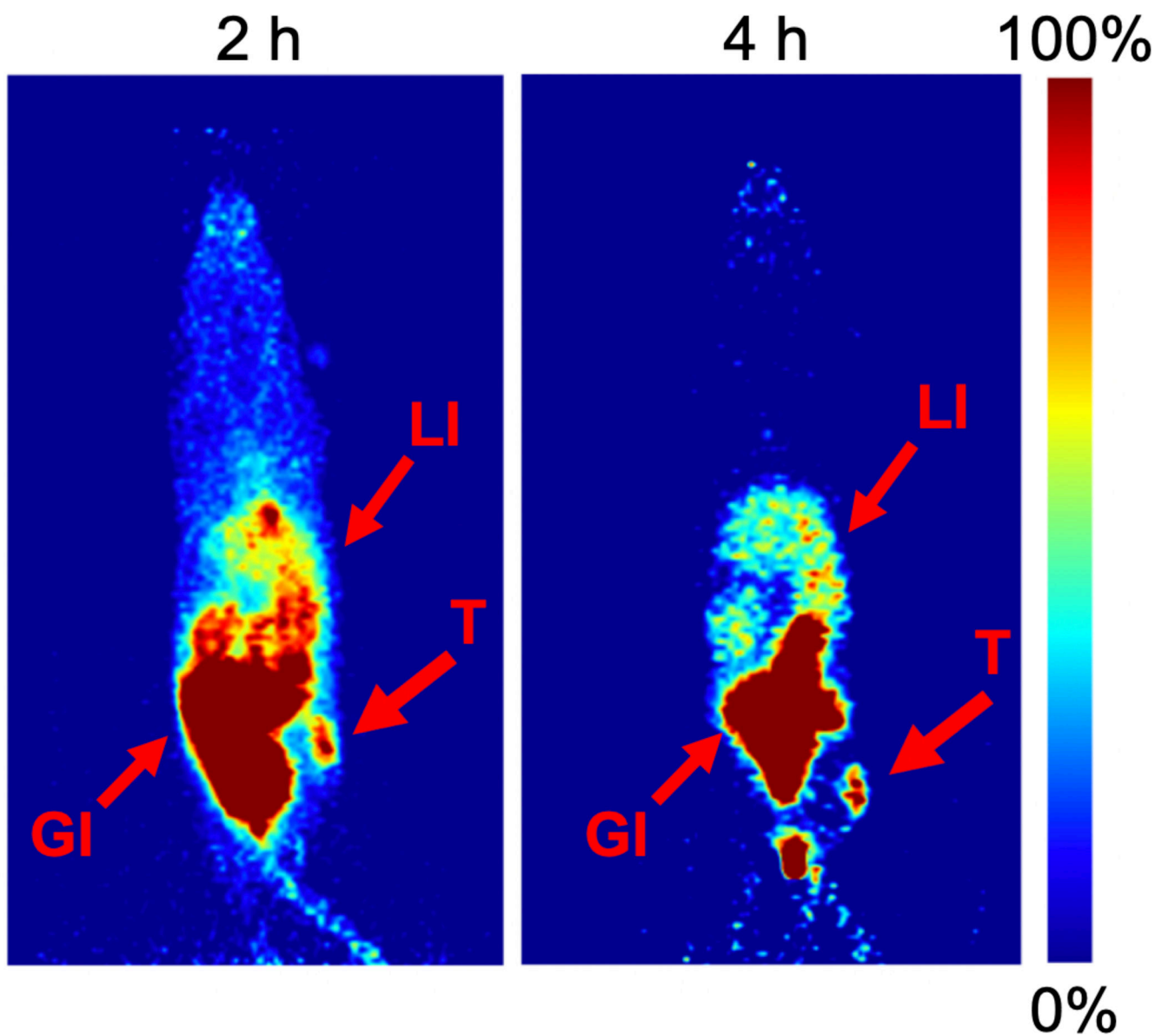
FIGURE 5.
Maximum intensity projection images of female BxPC3 xenografted nude mice administered with CB7-M5A 72 hours prior to $[^{68}Ga]$Ga-NOTA-PEG$_3$-NMe$_2$-Fc. The time values represent the amount of time after the radioligand administration and the arrows indicate the location of tumor (T), liver (LI) and gastrointestinal tract (GI). In order to visualize the tumor at both timepoints, different thresholds were used for displaying the image.